

# Probabilistic assessment of the seismic performance of earth slopes

Ellen M. Rathje · Yubing Wang · Peter J. Stafford ·  
George Antonakos · Gokhan Saygili

Received: 5 February 2013 / Accepted: 29 June 2013 / Published online: 18 July 2013  
© Springer Science+Business Media Dordrecht 2013

**Abstract** Sliding block displacements are used to evaluate the potential for seismic slope instability. Deterministic approaches are typically used to predict the expected level of sliding block displacement, although they do not rigorously account for uncertainties in the expected ground shaking, dynamic response, or displacement prediction. As a result, there is no concept of the actual hazard associated with the displacement computed by the deterministic approach. This paper summarizes and extends recent developments related to the probabilistic assessment of sliding block displacements. The probabilistic approach generates a hazard curve for displacement in which the annual rate of exceedance for a range of displacement levels is computed. The probabilistic approach is formulated both in terms of scalar hazard analysis (i.e., using one ground motion parameter, peak ground acceleration) and vector hazard analysis (i.e., using two ground motion parameters, peak ground acceleration and peak ground velocity), and applied both to rigid and flexible sliding block conditions. Generally, the vector probabilistic approach predicts displacements that are 2–3 times smaller than the scalar probabilistic approach, revealing the value of characterizing frequency content via peak ground velocity. Comparisons between the deterministic and probabilistic approaches, in either a scalar or vector context, indicate that the deterministic approach can severely underestimate displacements relative to the probabilistic approach because it ignores the aleatory variabilities in the dynamic and sliding responses of the sliding mass. This under-prediction is most significant for longer period sliding masses. Modifications to the deterministic approach

---

E. M. Rathje (✉) · Y. Wang  
Department of Civil, Architectural and Environmental Engineering, University of Texas at Austin,  
301 E. Dean Keeton St, Stop C1700, Austin, TX 78712, USA  
e-mail: e.rathje@mail.utexas.edu

P. J. Stafford  
Imperial College London, London, UK

G. Antonakos  
O.T.M. SA Consulting Engineering Company, Athens, Greece

G. Saygili  
University of Texas at Tyler, Tyler, TX, USA

are proposed that provide displacements that are more consistent with the probabilistic approach.

**Keywords** Seismic slope stability · Sliding displacements · Probabilistic · Slope performance

## 1 Introduction

The seismic performance of slopes is typically evaluated based on the sliding displacement predicted to occur along a critical sliding surface. This displacement represents the cumulative, downslope movement of a sliding mass due to earthquake shaking. The magnitude of sliding displacement relates well with observations of seismic performance of slopes (e.g., [Jibson et al. 2000](#)), and thus has been a useful parameter in seismic design and hazard assessment.

The magnitude of sliding displacement is strongly affected by the intensity, frequency content, and duration of earthquake shaking. Various empirical models are available that predict sliding displacement as a function of ground motion parameters and site parameters, but these models have significant aleatory variability (i.e., large standard deviation) such that a large range of displacements is predicted for a set of input parameters. Earthquake ground motions also display significant aleatory variability, yet current evaluation procedures for computing sliding displacement are based on a deterministic approach, in which the aleatory variability in the expected ground motion, dynamic response, and predicted displacement are either ignored or not treated rigorously. Thus, there is no concept of the actual hazard associated with the displacement computed by the deterministic approach. A probabilistic assessment of sliding displacement can account rigorously for the aleatory variability in earthquake ground shaking and in the dynamic response and sliding displacement predictions, providing a more complete assessment of the risk associated with seismic slope failure. It should be noted that the probabilistic framework presented here does not include epistemic uncertainty (e.g., uncertainty in the shear strength and shear stiffness of the soil in the slope). The effect of epistemic uncertainty on predicting slope displacements can be included through conventional logic tree approaches.

This paper summarizes and extends recent developments related to the probabilistic assessment of sliding displacements of slopes under seismic shaking. Newly developed models are presented that predict the dynamic response and sliding displacement of sliding masses and take advantage of multiple ground motion parameters. The value of these additional ground motion parameters in predicting sliding displacement is demonstrated. Probabilistic frameworks to predict the dynamic response and sliding displacement of slopes are introduced. The probabilistic frameworks are formulated both in terms of scalar hazard analysis (i.e., using one ground motion parameter) and vector hazard analysis (i.e., using two ground motion parameters). The probabilistic frameworks are applied to hypothetical examples, and the probabilistic results compared with deterministic results. The paper first considers rigid sliding masses, and then extends the approaches to flexible sliding masses.

## 2 Rigid sliding masses

### 2.1 Predictive models for the displacement of rigid sliding masses

Shallower and/or stiffer sliding masses subjected to low frequency seismic shaking respond as rigid bodies for which the dynamic response of the material within the sliding mass can be ignored (Fig. 1). The seismic loading for a rigid sliding mass is simply the acceleration–time ( $a-t$ ) history at the base of the sliding mass, with the destabilizing force-time history acting on the slope,  $F(t)$ , equal to the  $a-t$  history (in units of gravity,  $g$ ) times the weight of the sliding mass. The resistance to sliding is characterized by the yield acceleration,  $k_y$ , of the slope ( $k_y =$  seismic coefficient that when multiplied by the weight of the sliding mass and statically applied to the slope yields a factor of safety of 1.0). Earthquake-induced sliding displacements ( $D$ ) are expected if the peak ground acceleration (PGA), which is proportional to the maximum destabilizing force, exceeds the yield acceleration.

To calculate the sliding displacement of a rigid sliding mass, a suite of recorded  $a-t$  histories can be selected and numerically integrated for the sliding episodes that initiate when  $k_y$  is exceeded (in the destabilizing direction). Alternatively, an empirical model can be used that predicts  $D$  as a function of the yield acceleration and various ground motion parameters, such as the PGA, peak ground velocity (PGV), Arias Intensity ( $I_a$ ), etc. To be useful for probabilistic analyses empirical models for sliding displacement must provide estimates of both the median displacement and its standard deviation, and the most efficient models attempt to minimize the standard deviation (Cornell and Luco 2001).

Various empirical models for sliding displacement have been published in the literature (e.g., Bray and Travararou 2007; Jibson 2007), but this paper focuses on the models of Saygili and Rathje (2008) and Rathje and Saygili (2009). These models (hereafter called SR08/RS09) were developed from displacements computed using over 2,000 recorded motions from the Next Generation Attenuation (NGA) database. These models are used because they considered the ground motion parameters and combinations of ground motion parameters that minimize the standard deviation of the prediction of displacement (i.e.,  $\sigma_{lnD}$ ). Nonetheless, other displacement models can easily be implemented within the presented probabilistic

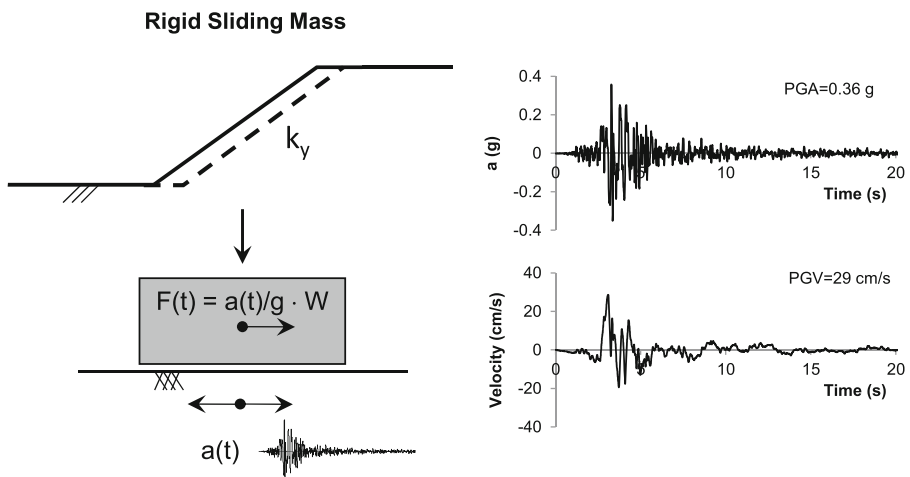


Fig. 1 Seismic loading parameters for rigid sliding masses

**Table 1** Parameters for (PGA, M) and (PGA, PGV) models

Parameter	(PGA, M) model	(PGA, PGV) model
$a_1$	4.89	-1.56
$a_2$	-4.85	-4.58
$a_3$	-19.64	-20.84
$a_4$	42.49	44.75
$a_5$	-29.06	-30.50
$a_6$	0.72	-0.64
$a_7$	0.89	1.55

approach. The work by Saygili and Rathje (2008) and Rathje and Saygili (2009) recommend two models: one model that uses a single ground motion parameter plus earthquake magnitude (i.e., the (PGA, M) model) and another model that uses two ground motion parameters (i.e., the (PGA, PGV) model). These models predict displacement in cm and assume a log-normal distribution for displacement. They are summarized in Eqs. (1) and (2) and in Table 1.

$$\ln D = a_1 + a_2 \left( \frac{k_y}{PGA} \right) + a_3 \left( \frac{k_y}{PGA} \right)^2 + a_4 \left( \frac{k_y}{PGA} \right)^3 + a_5 \left( \frac{k_y}{PGA} \right)^4 + a_6 \ln(PGA) + a_7 (M - 6) \tag{1a}$$

$$\sigma_{\ln D(PGA,M)} = 0.73 + 0.79 \left( \frac{k_y}{PGA} \right) - 0.54 \left( \frac{k_y}{PGA} \right)^2 \tag{1b}$$

$$\ln D = a_1 + a_2 \left( \frac{k_y}{PGA} \right) + a_3 \left( \frac{k_y}{PGA} \right)^2 + a_4 \left( \frac{k_y}{PGA} \right)^3 + a_5 \left( \frac{k_y}{PGA} \right)^4 + a_6 \ln(PGA) + a_7 \ln(PGV) \tag{2a}$$

$$\sigma_{\ln D(PGA,PGV)} = 0.41 + 0.52 \left( \frac{k_y}{PGA} \right) \tag{2b}$$

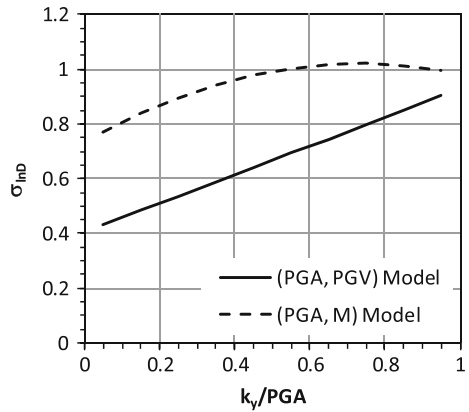
The (PGA, M) model is considered a scalar model because it uses only a single ground motion parameter. The (PGA, PGV) model is considered a vector model because it uses a vector of two ground motion parameters.

The standard deviations ( $\sigma_{\ln D}$ ) of both models were found to depend on  $k_y/PGA$ , with larger values of  $\sigma_{\ln D}$  occurring at larger values of  $k_y/PGA$ . The  $k_y/PGA$ -dependence for  $\sigma_{\ln D}$  is plotted in Fig. 2 for the two models, with values ranging between 0.75 and 1.0 (in natural log units) for the (PGA, M) model and ranging between 0.4 and 0.9 for the (PGA, PGV) model. The smaller  $\sigma_{\ln D}$  at smaller  $k_y/PGA$  indicates that the information provided by PGV is most useful in reducing the prediction uncertainty when more of the a–t history is sampled during the sliding displacement calculation (i.e.,  $k_y \ll PGA$ ).

### 2.2 Probabilistic framework for rigid sliding displacement

A probabilistic assessment of sliding displacement predicts the annual rate of exceedance ( $\lambda$ ) of different levels of sliding displacement (e.g., Lin and Whitman 1986; Yegian et al. 1991a,b;

**Fig. 2** Standard deviations associated with (PGA, M) and (PGA, PGV) models



Ghahraman and Yegian 1996; Travararou et al. 2004; Rathje and Saygili 2008), in the same way that a probabilistic seismic hazard analysis (PSHA) predicts  $\lambda$  for different levels of PGA or spectral acceleration. Thus, a seismic hazard curve for sliding displacement is a plot of  $\lambda_D$  versus  $D$ . The subscript  $D$  is used to distinguish the  $\lambda$  associated with displacement from the  $\lambda$  associated with ground motion.

Calculating  $\lambda_D$  requires knowledge of the probability that a displacement level is exceeded given a ground motion level and the annual probability of occurrence of that ground motion level. The product of these probabilities is computed and then integrated over all levels of ground motion to compute  $\lambda_D$ . For the (PGA, M) model, the calculation of  $\lambda_D(x)$ , where  $x$  is the displacement level, is given by:

$$\lambda_D(x) = \sum_i \sum_k P[D > x | \text{PGA}_i, M_k] \cdot P[M_k | \text{PGA}_i] \cdot P[\text{PGA}_i] \tag{3}$$

In Eq. (3)  $P[D > x | \text{PGA}_i, M_k]$  represents the probability that  $D > x$  given acceleration level  $\text{PGA}_i$  and earthquake magnitude  $M_k$ , and is computed from the model-predicted median displacement, its standard deviation, and the assumption of lognormality for these conditional displacements.  $P[M_k | \text{PGA}_i]$  is the conditional probability of occurrence of  $M_k$  given  $\text{PGA}_i$ , and is derived from the hazard disaggregation for each  $\text{PGA}_i$ . Finally,  $P[\text{PGA}_i]$  is the annual probability of occurrence of acceleration level  $\text{PGA}_i$  (i.e., a bin of PGA centered about  $\text{PGA}_i$ ) and is derived from differencing of the PGA hazard curve. The double summation represents numerical integration over bins for PGA and M. Equation (3) is easily implemented with information from a traditional PSHA for PGA.

It is worth noting that the rare-event assumption is employed when computing  $P[\text{PGA}_i]$  from the hazard curve. Assuming that the event under consideration is rare, the chance of two or more occurrences of the event within the time period of interest is small and thus the annual rate and the annual probability of exceedance are the same. Using this assumption, the annual probability that the acceleration level will fall within a bin of PGA centered about  $\text{PGA}_i$  (i.e.,  $P[\text{PGA}_i]$ ) can be approximated from the hazard values using:

$$P[\text{PGA}_i] = \lambda_{i-1/2} - \lambda_{i+1/2} = \frac{\lambda_i + \lambda_{i-1}}{2} - \frac{\lambda_i + \lambda_{i+1}}{2} = \frac{\lambda_{i-1} - \lambda_{i+1}}{2} \tag{4}$$

where  $\lambda_{i-1/2}$  and  $\lambda_{i+1/2}$  represent the hazard associated with PGA values halfway between adjacent PGA values in the hazard curve (i.e.,  $\text{PGA}_{i-1}$ ,  $\text{PGA}_i$ , and  $\text{PGA}_{i+1}$ ), and  $\lambda_{i-1}$ ,  $\lambda_i$ ,

and  $\lambda_{i+1}$  the hazard associated with the same adjacent PGA values. Note that the above expression assumes a linear variation of hazard values over the PGA bin and that the PGA probabilities estimated in this way will tend to exact values as the bin size reduces. In the case that large PGA bins are used then this approximation should be revisited to account for the nonlinear variation of hazard values over the bin.

For the (PGA, PGV) model, the calculation of  $\lambda_D(x)$  is given by:

$$\lambda_D(x) = \sum_i \sum_j P[D > x | \text{PGA}_i, \text{PGV}_j] \cdot P[\text{PGA}_i, \text{PGV}_j] \quad (5)$$

where  $P[D > x | \text{PGA}_i, \text{PGV}_j]$  represents the probability that  $D > x$  given ground motion levels  $\text{PGA}_i$  and  $\text{PGV}_j$ , and  $P[\text{PGA}_i, \text{PGV}_j]$  is the joint annual probability of occurrence of ground motion levels  $\text{PGA}_i$  and  $\text{PGV}_j$ . The double summation again represents integration and is performed over bins for both PGA and PGV.  $P[\text{PGA}_i, \text{PGV}_j]$  is computed via vector PSHA (VPSHA, [Bazzurro and Cornell 2002](#)). In addition to ground motion prediction models for PGA and PGV, VPSHA requires an estimate of the correlation coefficient between these two ground motion parameters. For PGA and PGV, the correlation coefficient ( $\rho$ ) has been estimated as 0.6 ([Rathje and Saygili 2008](#); [Baker 2007](#)). Currently, no commercially available PSHA software performs VPSHA calculations; however  $P[\text{PGA}_i, \text{PGV}_j]$  can be computed from the output of a traditional PSHA using:

$$P[\text{PGA}_i, \text{PGV}_j] = P[\text{PGV}_j | \text{PGA}_i] \cdot P[\text{PGA}_i] \quad (6)$$

$$P[\text{PGV}_j | \text{PGA}_i] = \sum_k \sum_l P[\text{PGV}_j | \text{PGA}_i, M_k, R_l] \cdot P[M_k, R_l | \text{PGA}_i] \quad (7)$$

These equations require a traditional PSHA for PGA that is used to compute  $P[\text{PGA}_i]$  and the associated magnitude/distance disaggregation to compute  $P[M_k, R_l | \text{PGA}_i]$ . Additionally, ground motion prediction equations for PGA and PGV, along with the correlation coefficient, are required to compute  $P[\text{PGV}_j | \text{PGA}_i, M_k, R_l]$ . Additional information can be found in [Bazzurro \(1998\)](#) and [Rathje and Saygili \(2009\)](#).

The framework presented in this section can be applied to other empirical displacement prediction models that use different ground motion parameters. In these cases, the appropriate ground motion parameters should be substituted in Eqs. (3) through (7). Applying this framework requires ground motion prediction equations for the ground motion parameters, the correlation coefficient between these ground motion parameters (if the vector approach is used), and a displacement prediction model with a robust estimate of  $\sigma_{\ln D}$ . No matter the empirical displacement model, the probabilistic framework can be implemented easily in a spreadsheet or any common numerical software package (e.g., Matlab).

### 2.3 Comparison of probabilistic and deterministic displacement predictions

To demonstrate the probabilistic approach, consider a site in Northern California with the PGA and PGV hazard curves shown in Fig. 3. The hazard curves were computed using the PSHA code and fault models of Abrahamson (personal communication) along with the [Boore and Atkinson \(2008\)](#) ground motion prediction equation and  $V_{s30} = 760$  m/s. The hazard at this site is significant, with  $\text{PGA} = 0.54$  g and  $\text{PGV} = 42$  cm/s at a 10% probability of exceedance in 50 years ( $\lambda = 0.0021$  1/year) and  $\text{PGA} = 0.88$  g and  $\text{PGV} = 71$  cm/s at a 2% probability of exceedance in 50 years ( $\lambda = 0.0004$  1/year). The disaggregations with respect to magnitude for PGA and PGV both indicate mean magnitudes of about 6.75 for these

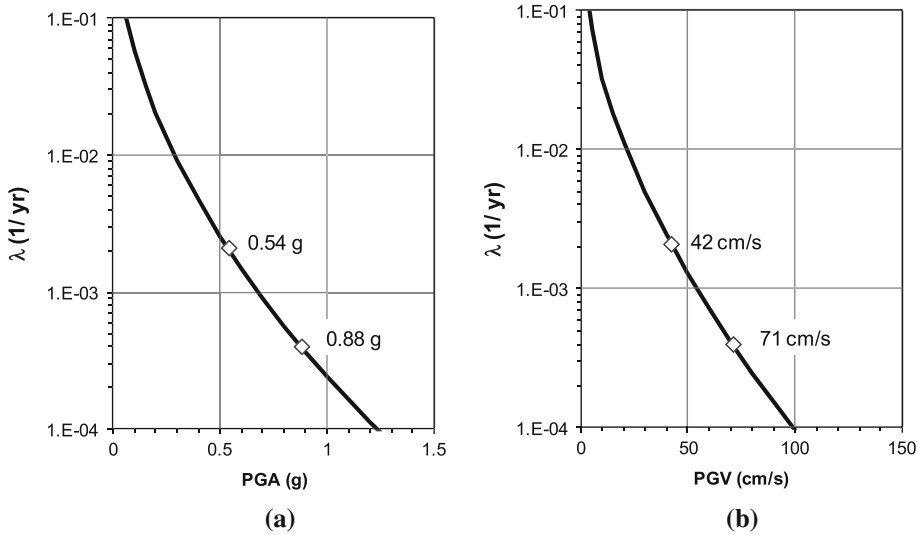
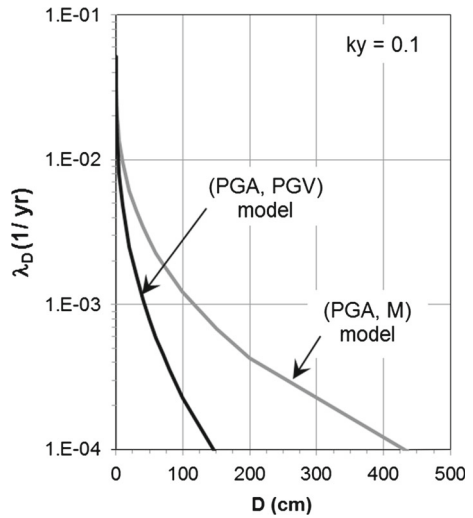


**Fig. 3** a PGA hazard curve and b PGV hazard curve used in analyses

**Fig. 4** Predicted displacement hazard curves using the (PGA, M) and (PGA, PGV) model



hazard levels. VPSHA was also performed for the site using the VPSHA code of Abrahamson (personal communication).

Displacement hazard curves were computed for a slope at the site with  $k_y = 0.1$  (Fig. 4). These curves were computed using the scalar (PGA, M) model and associated hazard information, as well as the vector (PGA, PGV) model and its relevant hazard information. Because of smaller median displacements and a smaller standard deviation, the (PGA, PGV) model predicts substantially smaller displacements than the (PGA, M) model at each hazard level. The difference can be as large as a factor of 3, indicating the value of including PGV in displacement predictions.

**Table 2** Probabilistic and deterministic displacement predictions for rigid sliding

$\lambda_D$ (1/year)*	Displacement comparisons ( $k_y = 0.1$ )			
	(PGA, M) model		(PGA, PGV) model	
	Probabilistic (cm)	Deterministic (cm)	Probabilistic (cm)	Deterministic (cm)
0.0021	67	43	25	29
0.0004	208	113	75	81

\*  $\lambda_D = 0.0021$  and  $0.0004$  represent 10 % and 2 % probabilities of exceedance in 50 years, respectively

Figure 4 can be used to identify the displacement that has a specific annual rate of exceedance (i.e.,  $\lambda_D$ ) or the probability of exceedance within a given time period if a Poisson assumption is adopted. The identified displacement levels for  $\lambda_D = 0.0021$  and  $0.0004$  1/year (i.e., 10 and 2 % probabilities of exceedance in 50 years) are listed in Table 2. As expected, the displacements at the smaller  $\lambda_D$  (i.e., smaller probability of exceedance) are larger than those at larger  $\lambda_D$  because larger displacements are less likely to occur. The displacement levels in Table 2 are associated with known hazard levels, making them the appropriate values to consider in design decisions.

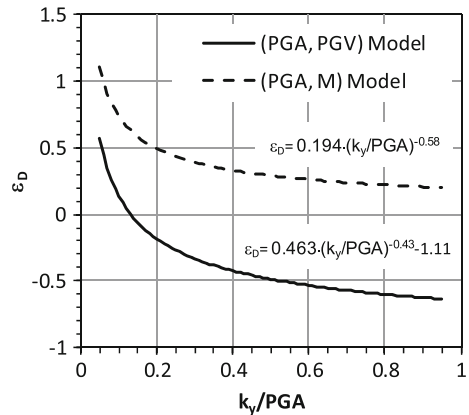
In practice, engineers generally consider a ground motion amplitude at a given hazard level and then make a deterministic prediction of displacement, rather than evaluating a displacement associated with a given hazard level. Typically, a deterministic displacement prediction represents the median displacement, although a  $+1\sigma$  displacement or an upper bound displacement may be considered in an effort to take into account some uncertainty in the displacement prediction. Table 2 lists the median deterministic displacements calculated using the (PGA, M) and (PGA, PGV) models. For the (PGA, M) model, the 10 and 2 % in 50 year values of PGA (Fig. 3a) were used along with the mean magnitude of 6.75 to compute the median deterministic displacement for  $k_y = 0.1$ . For the (PGA, PGV) model, the 10 and 2 % in 50 year values of PGA (Fig. 3a) and PGV (Fig. 3b) were used to compute the median deterministic displacement. The values in Table 2 show that for the (PGA, M) model, the deterministic approach significantly under-predicts displacement relative to the fully probabilistic value. This under-prediction is caused by the deterministic approach ignoring the uncertainty in the displacement prediction. On the other hand, the deterministic approach using the (PGA, PGV) model predicts displacements similar to or slightly larger than the fully probabilistic approach. As noted in Rathje and Saygili (2011), this result occurs because the probabilistic approach incorporates the correlation between PGA and PGV ( $\rho \sim 0.6$ ) while the deterministic approach uses PGA and PGV from separate hazard curves, which essentially assumes perfect correlation ( $\rho \sim 1.0$ ). Thus, the PGV is overestimated relative to PGA in the deterministic approach and this over-prediction in ground motion balances out, or is even larger than, the effect of ignoring the uncertainty in the displacement prediction.

Rathje and Saygili (2011) investigated the difference between probabilistic and deterministic displacements for a range of  $k_y$  values using the ground motion hazard at 12 sites in California. The goal of that study was to recommend what level of epsilon (i.e.,  $\epsilon_D$  = number of standard deviations) is required for the deterministic approach to predict displacements similar to the probabilistic approach. This value of  $\epsilon_D$  can be used with Eq. (8) to predict hazard-consistent levels of displacement:

$$D_{\text{hazard-consistent}} = \exp [\ln (D_{\text{median}}) + \epsilon_D \cdot \sigma_{\ln D}] \quad (8)$$



**Fig. 5** Recommended  $\varepsilon_D$  to use in deterministic displacement analyses to generate displacements consistent with probabilistic analyses



In Eq. (8), the median displacement is predicted using Eqs. (1a) or (2a) and the PSHA-derived ground motion values. The standard deviation in Eq. (8) is computed from Eqs. (1b) or (2b). Rathje and Saygili (2011) found that  $\varepsilon_D$  varied with  $k_y/PGA$ , as shown in Fig. 5, with  $\varepsilon_D$  decreasing with increasing  $k_y/PGA$ . Larger  $\varepsilon_D$  values are recommended for the (PGA, M) model than for the (PGA, PGV) model. The smaller values of  $\varepsilon_D$  indicate that the probabilistic and deterministic approaches predict more comparable levels of displacement for the (PGA, PGV) model than for the (PGA, M) model. As previously noted, this result is caused by the fact that the deterministic approach using the (PGA, PGV) model overestimates the correlated values of (PGA, PGV), which counteracts the effect of ignoring displacement uncertainty. This effect even makes  $\varepsilon_D$  negative for the (PGA, PGV) model over a large range of  $k_y/PGA$  values (Fig. 5).

### 3 Flexible sliding masses

#### 3.1 Predictive models for the dynamic response of flexible sliding masses

Deeper and/or softer sliding masses subjected to high frequency input signals behave as flexible bodies such that the rigid block model is not appropriate. In these cases, the dynamic response of the flexible sliding mass must be taken into account (Fig. 6). Two-dimensional finite element analysis can be used to model this dynamic response, or alternatively the sliding mass at its maximum thickness can be modeled as a one-dimensional soil column. Previous research (e.g., Rathje and Bray 2001, Vrymoed and Calzascia 1978) has shown that the one-dimensional simplification provides an adequate estimate of the seismic loading for deeper sliding masses. A decoupled sliding block analysis (e.g., Makdisi and Seed 1978) uses the results of the dynamic response analysis to compute the sliding displacement. The seismic loading time history for the sliding mass is related to the seismic coefficient ( $k$ )-time history, in which  $k$  represents the average acceleration within the sliding mass. The destabilizing force-time history ( $F(t)$ ) is then simply equal to the  $k$ -time history times the weight of the sliding mass. Earthquake-induced sliding displacements are expected if the maximum seismic coefficient ( $k_{max}$ ) exceeds the yield acceleration,  $k_y$ , of the slope (Fig. 6).

To calculate the sliding displacement of a flexible sliding mass, a suite of recorded  $a-t$  histories can be selected and used as input into one-dimensional wave propagation analysis

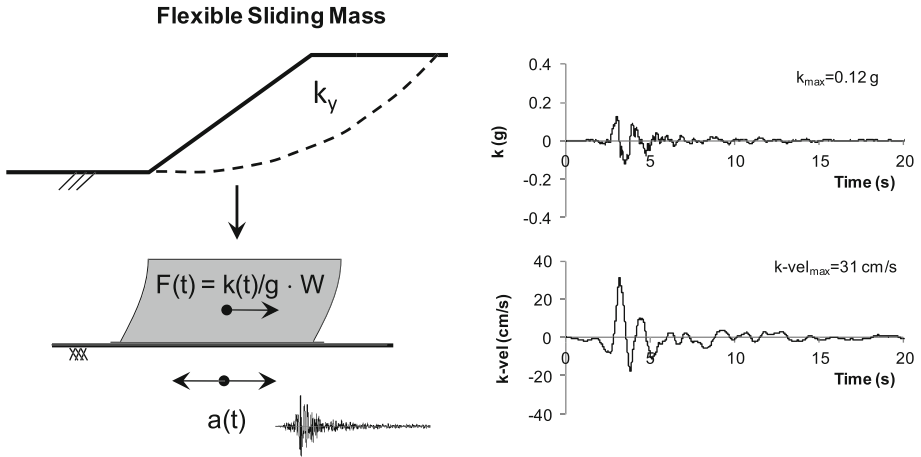


**Fig. 6** Seismic loading parameters for flexible sliding masses

to compute  $k$ -time histories for the sliding mass. Each  $k$ -time history can then be numerically integrated for the sliding episodes that initiate when  $k_y$  is exceeded. Alternatively, empirical models (e.g., Makdisi and Seed 1978; Bray and Rathje 1998) can be used that first predict  $k_{max}$  as a function of ground shaking and site characteristics, and then predict  $D$  as a function of  $k_y$  and  $k_{max}$ . Other empirical models are available (e.g., Bray and Travararou 2007) that predict  $D$  for flexible sliding masses directly from the ground motion and site characteristics.

The empirical models for rigid sliding indicate that PGV improves the displacement prediction, and it follows that an analogous parameter should be defined for flexible sliding masses. If the  $k$ -time history for flexible sliding is analogous to the  $a$ - $t$  history for rigid sliding, then the numerical integration of the  $k$ -time history is analogous to the numerical integration of the  $a$ - $t$  history (i.e., the velocity time history). The velocity that is computed by numerical integration of the  $k$ -time history is called  $k$ -vel (Rathje and Antonakos 2011), and it provides information regarding the frequency content of the  $k$ -time history. The maximum of the  $k$ -vel—time history is  $k\text{-vel}_{max}$ . The parameters  $k_{max}$  and  $k\text{-vel}_{max}$  represent the dynamic response of a sliding mass, and empirical models have been developed that predict these parameters as a function of the ground shaking and site characteristics (Rathje and Antonakos 2011). These models were developed through one-dimensional site response analyses where  $k_{max}$  and  $k\text{-vel}_{max}$  were computed at the base of different sliding masses subjected to 80 input motions. The predictive models for  $k_{max}$  and  $k\text{-vel}_{max}$  are summarized below.

The model for  $k_{max}$  predicts  $\ln(k_{max}/PGA)$  as a function of  $\ln(T_s/T_m)$  and  $PGA$ , where  $T_s$  is the natural period of the sliding mass and  $T_m$  (Rathje et al. 2004) is the mean period of the earthquake motion:

For  $T_s/T_m \geq 0.1$ :

$$\ln\left(\frac{k_{max}}{PGA}\right) = (0.459 - 0.702 \cdot PGA) \cdot \ln\left\{\left(\frac{T_s}{T_m}\right)\right\} + (-0.228 + 0.076 \cdot PGA) \cdot \left(\ln\left\{\left(\frac{T_s}{T_m}\right)\right\}\right)^2 \tag{9}$$

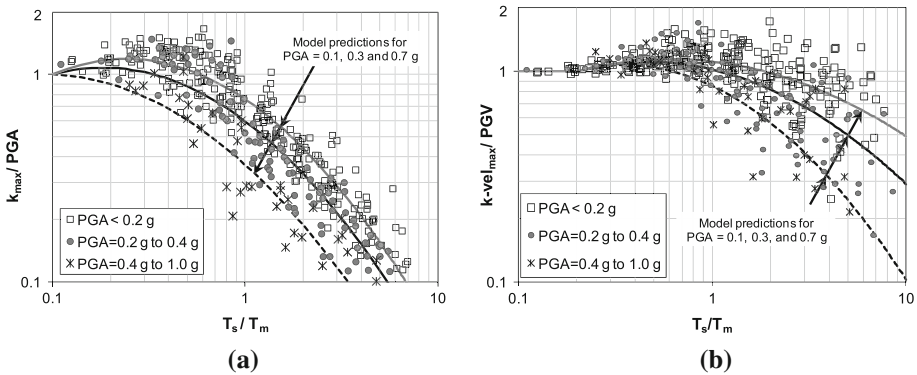


**Fig. 7** Predictive models for the dynamic response of flexible sliding masses: **a**  $k_{\max}$  and **b**  $k\text{-vel}_{\max}$

For  $T_s / T_m < 0.1$ :

$$\ln \left( \frac{k_{\max}}{\text{PGA}} \right) = 0.0$$

The standard deviation for this model in natural log units is 0.25. Given  $T_s / T_m$  and the input motion PGA,  $k_{\max}$  is computed from the predicted value of  $k_{\max} / \text{PGA}$  multiplied by the input motion PGA. The model predictions from Eq. (9) are shown in Fig. 7a for  $\text{PGA} = 0.1, 0.3, \text{ and } 0.7 \text{ g}$ . The model predicts a parabolic relationship between  $k_{\max} / \text{PGA}$  and  $T_s / T_m$  in log-log space, with the shape of this relationship varying with PGA. Smaller values of  $k_{\max} / \text{PGA}$  are predicted at larger PGA and larger  $T_s / T_m$ . At  $T_s / T_m \leq 0.1$  the relationship predicts  $k_{\max} = \text{PGA}$ , which indicates rigid sliding conditions.

The model for  $k\text{-vel}_{\max}$  predicts  $\ln(k\text{-vel}_{\max} / \text{PGV})$  as a function of  $\ln(T_s / T_m)$  and PGA, and is given by:

For  $T_s / T_m \geq 0.2$ :

$$\ln \left( \frac{k\text{-vel}_{\max}}{\text{PGV}} \right) = (0.240) \cdot \ln \left\{ \left( \frac{T_s}{T_m} \right) \right\} + (-0.091 - 0.171 \cdot \text{PGA}) \cdot \left( \ln \left\{ \left( \frac{T_s}{T_m} \right) \right\} \right)^2 \quad (10)$$

For  $T_s / T_m < 0.2$ :

$$\ln \left( \frac{k\text{-vel}_{\max}}{\text{PGV}} \right) = 0.0$$

The standard deviation for this model in natural log units is 0.25. Given  $T_s / T_m$  and the input motion PGA and PGV,  $k\text{-vel}_{\max}$  is computed from the predicted value of  $k\text{-vel}_{\max} / \text{PGV}$  multiplied by the input motion PGV. The model predictions from Eq. (10) are shown in Fig. 7b for input  $\text{PGA} = 0.1, 0.3, \text{ and } 0.7 \text{ g}$ .  $k\text{-vel}_{\max}$  displays less nonlinearity than  $k_{\max}$ , with  $k\text{-vel}_{\max} / \text{PGV}$  maintaining values between 1.3 and 0.7 over a large range of  $T_s / T_m$ . Additionally, the period range over which  $k\text{-vel}_{\max} = \text{PGV}$  extends to  $T_s / T_m = 0.2$ .

### 3.2 Predictive models for the sliding displacement of flexible sliding masses

Rathje and Antonakos (2011) extended the displacement models of SR08/RS09 to make them applicable to flexible sliding masses. The extension involves using  $k_{max}$  and  $k\text{-vel}_{max}$  in lieu of PGA and PGV in the original (PGA, M) and (PGA, PGV) models, and the addition of a term that is a function of  $T_s$ . The modified models for flexible sliding displacement are given in Eq. (11) for the  $(k_{max}, M)$  model and Eq. (12) for the  $(k_{max}, k\text{-vel}_{max})$  model.

$$\ln D = a_1 + a_2 \left(\frac{k_y}{k_{max}}\right) + a_3 \left(\frac{k_y}{k_{max}}\right)^2 + a_4 \left(\frac{k_y}{k_{max}}\right)^3 + a_5 \left(\frac{k_y}{k_{max}}\right)^4 + a_6 \ln(k_{max}) + a_7(M - 6) + f_1(T_s) \tag{11a}$$

$$\text{with } f_1(T_s) = \begin{cases} 3.69 \cdot T_s - 1.22 \cdot T_s^2, & T_s \leq 1.5 \text{ s} \\ 2.78, & T_s > 1.5 \text{ s} \end{cases}$$

$$\sigma_{\ln D(k_{max}, M)} = 0.694 + 0.322 \left(\frac{k_y}{k_{max}}\right) \tag{11b}$$

$$\ln D = a_1 + a_2 \left(\frac{k_y}{k_{max}}\right) + a_3 \left(\frac{k_y}{k_{max}}\right)^2 + a_4 \left(\frac{k_y}{k_{max}}\right)^3 + a_5 \left(\frac{k_y}{k_{max}}\right)^4 + a_6 \ln(k_{max}) + a_7 \ln(k\text{-vel}_{max}) + f_2(T_s) \tag{12a}$$

$$\text{with } f_2(T_s) = \begin{cases} 1.42 \cdot T_s, & T_s \leq 0.5 \text{ s} \\ 0.71, & T_s > 0.5 \text{ s} \end{cases}$$

$$\sigma_{\ln D(k_{max}, k\text{-vel}_{max})} = 0.40 + 0.284 \left(\frac{k_y}{k_{max}}\right) \tag{12b}$$

The parameters  $a_1$  through  $a_7$  in Eqs. (11) and (12) are set equal to those developed previously for rigid sliding (Table 1). Note that the standard deviations for these models are given in Eqs. (11b) and (12b). These standard deviations are generally smaller than those for the rigid models.

Figure 8 shows the predicted  $k_{max}$ ,  $k\text{-vel}_{max}$ , and  $D$  as a function of  $T_s$  for ground shaking characterized by a deterministic  $M = 7$ ,  $R = 5$  km event with  $PGA = 0.35$  g,  $PGV = 30$  cm/s, and  $T_m = 0.45$  s.  $k_{max}$  (Fig. 8a) peaks at 0.37 g at a very short period of 0.075 s, and then decreases at longer periods. At  $T_s = 1.0$  s,  $k_{max}$  is equal to 0.1 g, which is less than one-third the value for  $T_s = 0.0$  s (i.e., rigid sliding).  $k\text{-vel}_{max}$  (Fig. 8b) reaches its peaks of 33 cm/s at a longer period ( $T_s \sim 0.25$  s), and decreases only to 22 cm/s at  $T_s = 1.0$  s. This value is about 75% of the value at  $T_s = 0.0$  s. The displacement predictions (Fig. 8c) show the displacement peaking at  $T_s$  between 0.1 and 0.2 s because it is over this period range where  $k_{max}$  and  $k\text{-vel}_{max}$  are amplified. Displacements generally decrease at larger values of  $T_s$  because  $k_{max}$  decreases, and the displacements approach zero as  $k_{max}$  approaches  $k_y$ . Generally, the  $(k_{max}, k\text{-vel}_{max})$  model predicts displacements 2–3 times smaller than the  $(k_{max}, M)$  model because of the additional frequency content information provided by  $k\text{-vel}_{max}$ .

### 3.3 Probabilistic framework for flexible sliding displacements

Similar to rigid sliding displacements, calculating  $\lambda_D$  for flexible sliding involves calculating the probability that a displacement level is exceeded given a ground motion level and the annual probability of occurrence of that ground motion level. However, ground shaking is

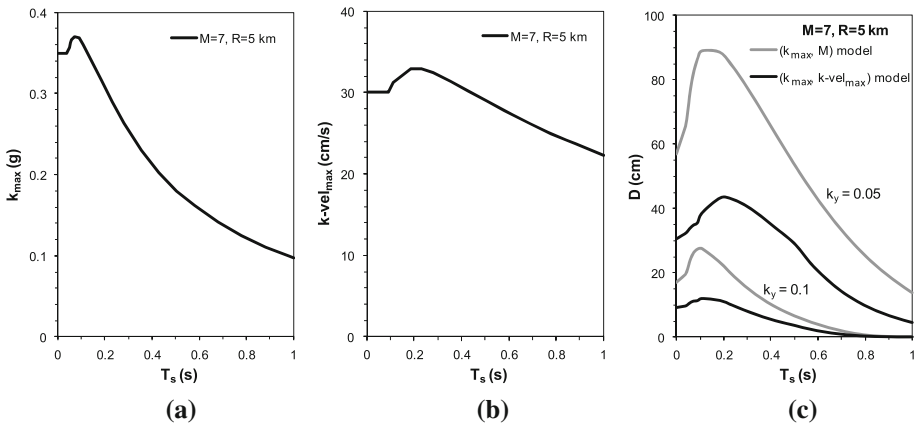


**Fig. 8** Predicted **a**  $k_{max}$ , **b**  $k\text{-vel}_{max}$ , and **c** sliding displacement as a function of the natural period of the sliding mass  $f$  or a  $M = 7, R = 5$  km event

characterized by  $k_{max}$  and  $k\text{-vel}_{max}$  for flexible sliding rather than by PGA and PGV. For the  $(k_{max}, M)$  model,  $\lambda_D$  is computed by:

$$\lambda_D(x) = \sum_k \sum_m P[D > x | k_{max_m}, M_k] \cdot P[k_{max_m}, M_k] \tag{13}$$

In Eq. (13)  $P[D > x | k_{max_m}, M_k]$  represents the probability of  $D > x$  given a  $k_{max}$  value of  $k_{max_m}$  and earthquake magnitude  $M_k$ , and it is computed from the model-predicted median displacement and its standard deviation (Eq. 11).  $P[k_{max_m}, M_k]$  is the joint annual probability of occurrence of  $k_{max_m}$  and  $M_k$ . This joint annual probability of occurrence is computed from the annual rate of occurrence of  $PGA_i$  (i.e.,  $P[PGA_i]$ ), the disaggregation for PGA (i.e.,  $P[M_k | PGA_i]$ ), and the probability that  $PGA_i$  will generate  $k_{max_m}$  (i.e.,  $P[k_{max_m} | PGA_i, M_k]$ ) using:

$$P[k_{max_m}, M_k] = \sum_i P[k_{max_m} | PGA_i, M_k] \cdot P[M_k | PGA_i] \cdot P[PGA_i] \tag{14}$$

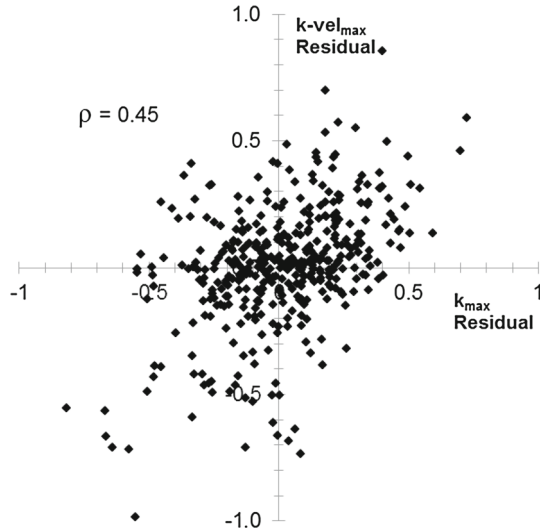
In Eq. (14),  $P[k_{max_m} | PGA_i, M_k]$  is derived from the predictive model for  $k_{max}/PGA$  and its standard deviation. The summation represents numerical integration over PGA. Although  $M$  does not influence the  $k_{max}$  prediction, it is required for the displacement prediction and therefore must be carried through the calculation. To simplify the calculations, Eq. (14) ignores the variation of  $T_m$  with magnitude and distance, and uses one value when computing  $k_{max}$ .

For the  $(k_{max}, k\text{-vel}_{max})$  model,  $\lambda_D$  is computed by:

$$\lambda_D(x) = \sum_m \sum_n P[D > x | k_{max_m}, k\text{-vel}_{max_n}] \cdot P[k_{max_m}, k\text{-vel}_{max_n}] \tag{15}$$

where  $P[D > x | k_{max_m}, k\text{-vel}_{max_n}]$  represents the probability of  $D > x$  given seismic loading levels  $k_{max_m}$  and  $k\text{-vel}_{max_n}$ , and  $P[k_{max_m}, k\text{-vel}_{max_n}]$  is the joint annual probability of occurrence of seismic loading levels  $k_{max_m}$  and  $k\text{-vel}_{max_n}$ .  $P[k_{max_m}, k\text{-vel}_{max_n}]$  is computed from  $P[PGA_i, PGV_j]$  and the probabilities of obtaining  $k_{max_m}$  and  $k\text{-vel}_{max_n}$  given  $PGA_i$  and  $PGV_j$  using:

**Fig. 9** Correlation between  $k\text{-vel}_{\max}$  and  $k_{\max}$



$$P[k_{\max_m}, k\text{-vel}_{\max_n}] = \sum_i \sum_j P[k_{\max_m} | k\text{-vel}_{\max_n}, \text{PGA}_i, \text{PGV}_j] \cdot P[k\text{-vel}_{\max_n} | \text{PGA}_i, \text{PGV}_j] \cdot P[\text{PGA}_i, \text{PGV}_j] \quad (16)$$

The predictive model for  $k\text{-vel}_{\max}$ /PGV and its standard deviation are used to compute  $P[k\text{-vel}_{\max_n} | \text{PGA}_i, \text{PGV}_j] \cdot P[k_{\max_m} | k\text{-vel}_{\max_n}, \text{PGA}_i, \text{PGV}_j]$  requires that the correlation between  $k_{\max}$  and  $k\text{-vel}_{\max}$  be considered. The correlation coefficient between  $k_{\max}$  and  $k\text{-vel}_{\max}$  is used to derive a conditional mean and standard deviation for  $k_{\max}$ , and these values are used to compute  $P[k_{\max_m} | k\text{-vel}_{\max_n}, \text{PGA}_i, \text{PGV}_j]$ .

To evaluate the correlation coefficient between  $k_{\max}$  and  $k\text{-vel}_{\max}$ , the residuals of the computed values of  $k_{\max}$  and  $k\text{-vel}_{\max}$  relative to the predictive models of Rathje and Antonakos (2011) were calculated and used to estimate the correlation coefficient. This approach is similar to the approach taken by Baker (2007) when considering the correlation between various ground motion parameters. The  $k_{\max}$  and  $k\text{-vel}_{\max}$  residuals are plotted in Fig. 9 and show moderate correlation. The computed correlation coefficient is 0.45.

Although not used explicitly in the calculation of the displacement hazard curve, it is illustrative to compute the hazard curves for  $k_{\max}$  and  $k\text{-vel}_{\max}$ . These hazard curves are computed independently of one another using:

$$\lambda_{k_{\max}}(y) = \sum_i \sum_k P[k_{\max} > y | \text{PGA}_i, M_k] \cdot P[M_k | \text{PGA}_i] \cdot P[\text{PGA}_i] \quad (17)$$

$$\lambda_{k\text{-vel}_{\max}}(z) = \sum_i \sum_j P[k\text{-vel}_{\max} > z | \text{PGA}_i, \text{PGV}_j] \cdot P[\text{PGA}_i, \text{PGV}_j] \quad (18)$$

### 3.4 Comparison of probabilistic and deterministic dynamic response and displacement predictions

To illustrate the probabilistic approach for flexible sliding the hazard information used for the same Northern California site (Fig. 3) is used. The mean period of the ground motion is deterministically set at  $T_m = 0.5$  s and calculations are made for  $T_s/T_m$  equal to 0.0, 0.25, 0.5,

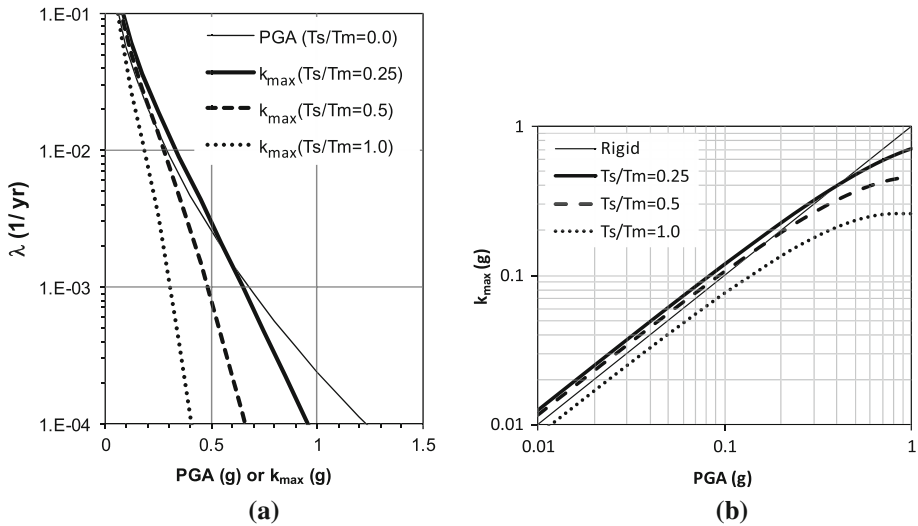


**Fig. 10** **a**  $k_{max}$  hazard curves and **b** variation of  $k_{max}$  with PGA from Eq. (9) for different values of  $T_s/T_m$

**Table 3** Probabilistic and deterministic  $k_{max}$  predictions

$\lambda$ (1/year)	$k_{max}$ comparisons					
	$T_s/T_m = 0.25$		$T_s/T_m = 0.5$		$T_s/T_m = 1.0$	
	Probabilistic (g)	Deterministic (g)	Probabilistic (g)	Deterministic (g)	Probabilistic (g)	Deterministic (g)
0.0021	0.55	0.50	0.42	0.38	0.27	0.24
0.0004	0.77	0.66	0.56	0.45	0.35	0.26

and 1.0. These conditions represent rigid sliding ( $T_s = 0$ ) and flexible sliding for  $T_s = 0.125, 0.25$  and  $0.5$  s. The dynamic response predictions, as well as the displacement predictions, are computed using the probabilistic and deterministic approaches. Note that assuming a larger value of  $T_m$  would result in a larger dynamic response and larger displacements.

The hazard curves for  $k_{max}$  are shown in Fig. 10a, along with the hazard curve for PGA (i.e., rigid conditions). The hazard curves for the three different values of  $T_s/T_m$  generally predict smaller values of seismic loading than for rigid conditions, except at the larger values of  $\lambda$  (i.e., shorter return periods). The seismic loading levels generally get smaller with increasing  $T_s/T_m$  because  $k_{max}$  generally decreases with  $T_s/T_m$  (Fig. 7). Figure 10b plots predicted values of  $k_{max}$  as a function of PGA for the three different values of  $T_s/T_m$ . Note that the median prediction of  $k_{max}$  is greater than PGA only for  $T_s/T_m \leq 0.5$  and for PGA smaller than about 0.2 g. Also, note that for  $T_s/T_m = 1.0$ ,  $k_{max}$  reaches a limiting value of 0.26 g and does not continue to increase for PGA larger than about 0.7 g.

Table 3 compares the probabilistic  $k_{max}$  values for 10 and 2% probabilities of exceedance in 50 years with those evaluated deterministically based on the 10 and 2% in 50 year values of PGA. The deterministic values are between 10 and 25% smaller than the probabilistic values because the probabilistic values take into account the uncertainty in the prediction of  $k_{max}$ . The difference is largest for  $T_s/T_m = 1.0$  because the deterministic values approach

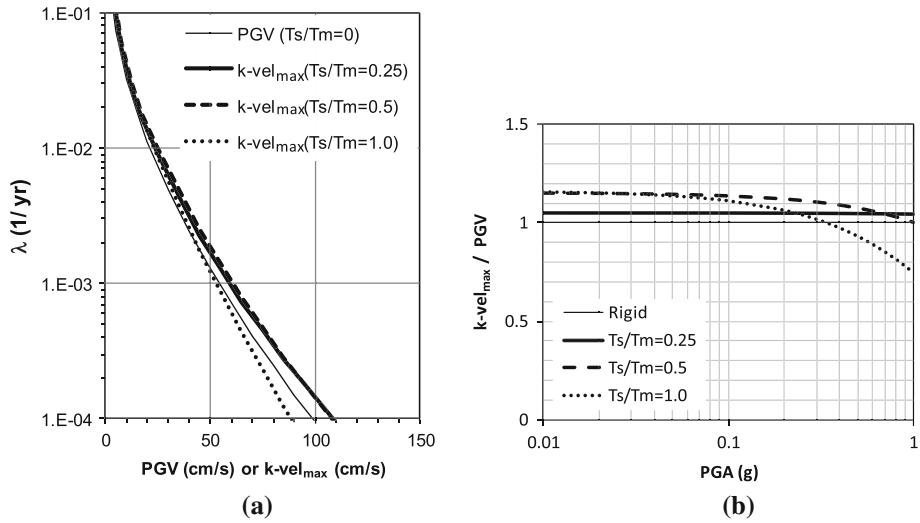


**Fig. 11** **a**  $k\text{-vel}_{\max}$  hazard curves and **b** variation of  $k\text{-vel}_{\max} / \text{PGV}$  with PGA for different values of  $T_s/T_m$

**Table 4** Probabilistic and deterministic  $k\text{-vel}_{\max}$  predictions

$\lambda$ (1/year)	$k\text{-vel}_{\max}$ comparisons					
	$T_s/T_m = 0.25$		$T_s/T_m = 0.5$		$T_s/T_m = 1.0$	
	Probabilistic (cm/s)	Deterministic (cm/s)	Probabilistic (cm/s)	Deterministic (cm/s)	Probabilistic (cm/s)	Deterministic (cm/s)
0.0021	46	45	48	46	43	39
0.0004	77	74	78	72	66	56

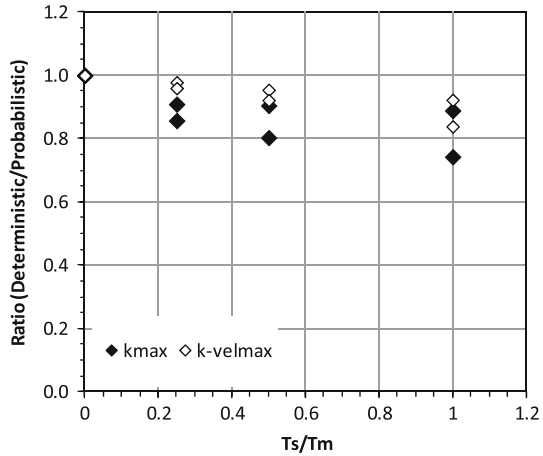
the limiting value of 0.26 g, while the probabilistic values continue to increase due to the variability in the  $k_{\max}$  prediction.

The  $k\text{-vel}_{\max}$  hazard curves are shown in Fig. 11a, along with the hazard curve for PGV (i.e., rigid conditions). The  $k\text{-vel}_{\max}$  hazard curves closely follow the PGV hazard curve because  $k\text{-vel}_{\max}$  does not decrease quickly with increasing PGA or  $T_s/T_m$  (Fig. 11b). The probabilistic  $k\text{-vel}_{\max}$  values for 10 and 2% probabilities of exceedance in 50 years are shown in Table 4 along with those evaluated deterministically based on the 10 and 2% in 50 year values of PGA and PGV. The difference between the probabilistic and deterministic values of  $k\text{-vel}_{\max}$  is modest, with the deterministic values generally 5–10% smaller than the probabilistic values.

The ratio of deterministic predictions to probabilistic predictions in Table 4 is plotted versus  $T_s/T_m$  in Fig. 12 for  $k_{\max}$  and  $k\text{-vel}_{\max}$ . Here it is clearly observed that the deterministic predictions underestimate the probabilistic predictions, and the ratio decreases with increasing  $T_s/T_m$ . At a given  $T_s/T_m$ , the under-prediction is larger for  $k_{\max}$  than for  $k\text{-vel}_{\max}$  and the under-prediction is larger for smaller  $\lambda$ . The deterministic  $k\text{-vel}_{\max}$  values are relatively similar to the probabilistic predictions because the deterministic predictions of  $k\text{-vel}_{\max}$  are based on perfectly correlated ( $\rho \sim 1.0$ ) values of PGA and PGV, while the probabilistic  $k\text{-vel}_{\max}$  are based on  $\rho \sim 0.45$ . Therefore, although the deterministic values of  $k\text{-vel}_{\max}$



**Fig. 12** Ratio of deterministic to probabilistic predictions of  $k_{\max}$  and  $k\text{-vel}_{\max}$



ignore the uncertainty in the  $k\text{-vel}_{\max}$  prediction, the larger ground motion levels used in its deterministic calculation somewhat balances this issue out.

Displacement hazard curves for the Northern California site and  $k_y = 0.1$  are shown in Fig. 13. Displacement hazard curves are computed using the  $(k_{\max}, M)$  and  $(k_{\max}, k\text{-vel}_{\max})$  models, and curves are shown for rigid conditions as well as for the three  $T_s/T_m$  values. Similar to previous comparisons for rigid sliding, the  $(k_{\max}, k\text{-vel}_{\max})$  model predicts smaller displacements than the  $(k_{\max}, M)$  model. The difference is typically between a factor of 2 and 3, indicating the value of incorporating frequency content via  $k\text{-vel}_{\max}$  when making displacement predictions. For both of the models, flexible sliding block displacements are generally larger than rigid sliding block displacements for  $T_s/T_m = 0.25$  and  $0.5$ . At  $T_s/T_m = 1.0$ , the flexible sliding block displacements are smaller than the rigid sliding block displacements. The displacement hazard curves in Fig. 13 allow an engineer to easily identify the displacement levels associated with the hazard level of interest. For example, the  $(k_{\max}, k\text{-vel}_{\max})$  model for  $T_s/T_m = 0.25$  predicts a displacement of 33 cm at  $\lambda = 0.0021$  1/year (10% in 50 years) and 101 cm at  $\lambda = 0.0004$  1/year (2% in 50 years).

Having developed and demonstrated the probabilistic approach, it is useful again to compare probabilistic results with the results that would be obtained from traditional deterministic analysis. Deterministic analysis takes the ground motions (i.e., PGA and PGV) from a hazard curve for a given hazard level, uses these values to predict a median dynamic response (i.e.,  $k_{\max}$  and  $k\text{-vel}_{\max}$ ), and uses the median dynamic response to predict a median displacement. Deterministic and probabilistic analyses were performed for the Northern California site for  $k_y = 0.1$  and  $0.2$ , and  $T_s/T_m = 0.0, 0.25, 0.5$ , and  $1.0$  using the  $(k_{\max}, M)$  and  $(k_{\max}, k\text{-vel}_{\max})$  models. The ratio of the deterministic to probabilistic displacements is plotted versus  $T_s/T_m$  in Fig. 14 for all of the analyses performed. The displacement differences (i.e., probabilistic–deterministic) associated with the data in Fig. 14 are mostly between 10 and 100 cm for the  $(k_{\max}, M)$  model and between  $\pm 5$  cm for the  $(k_{\max}, k\text{-vel}_{\max})$  model. It is clear from the data in Fig. 14 that the deterministic analysis under-predicts displacement for almost all cases (except for  $T_s/T_m = 0.0$  using the vector model) and it severely under-predicts the displacements at larger  $T_s/T_m$ . The issue at larger  $T_s/T_m$  is that the deterministic prediction of  $k_{\max}$  may approach  $k_y$  such that very small deterministic displacements are predicted. In the probabilistic analysis all potential  $k_{\max}$  values (large and small) and their probability of occurrence are taken into account in

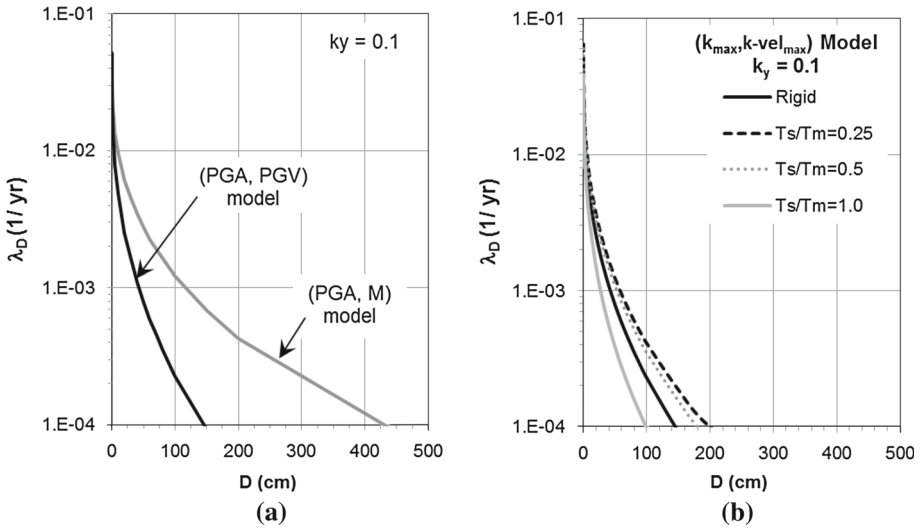
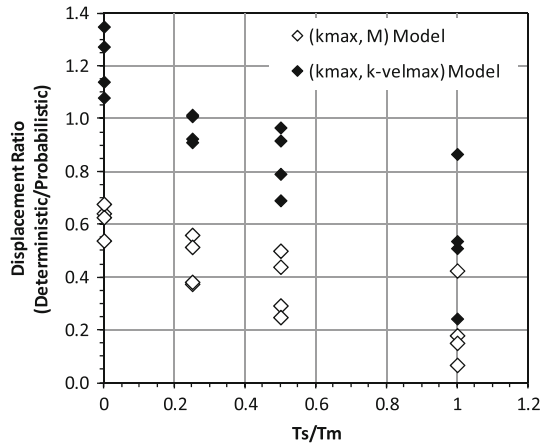


**Fig. 13** Displacement hazard curves for **a** ( $k_{max}$ , M) displacement model and **b** ( $k_{max}$ ,  $k\text{-vel}_{max}$ ) displacement model for different values of  $T_s/T_m$  and  $k_y = 0.1$

**Fig. 14** Ratio of deterministic to probabilistic predictions of displacements



the displacement calculation such that larger displacements are predicted for a given hazard level.

The data in Fig. 14 represents a small sample of analyses, but they indicate the potential un-conservatism in deterministic analysis and demonstrate the value of performing fully probabilistic analysis. As an alternative to fully probabilistic analysis, a modified deterministic approach may be developed that applies appropriate values of epsilon such that hazard-consistent displacements are generated. This approach would be similar to the approach developed by Rathje and Saygili (2011) for rigid sliding block analyses, but would require accounting for hazard consistent values of  $k_{max}$ ,  $k\text{-vel}_{max}$  as well as hazard-consistent displacement.

## 4 Conclusions

The probabilistic assessment of the seismic sliding displacements of slopes is a useful framework because it rationally takes into account the significant aleatory variabilities in the prediction of sliding displacement due to earthquake shaking. The probabilistic framework uses the output from a traditional PSHA and can be implemented within a spreadsheet or numerical software package, making it a tool that can be used easily by practicing engineers. The displacement hazard curve generated by the probabilistic analysis can be used to identify the displacement level associated with a specified hazard level (i.e., annual probability of exceedance). This allows the engineer to predict the performance for a known hazard level, rather than simply identifying the design motion based on a specified hazard level and predicting a deterministic displacement.

A vector hazard framework, which uses multiple ground motion parameters to describe seismic shaking (e.g., PGA and PGV or  $k_{\max}$  and  $k\text{-vel}_{\max}$ ), provides smaller estimates of sliding displacement than a scalar framework, which uses only a single ground motion parameter (e.g., PGA or  $k_{\max}$ ). The displacement from vector hazard analysis may be 2–3 times smaller than from scalar hazard analysis. This outcome results from accounting for frequency content in the input ground motion when PGV or  $k\text{-vel}_{\max}$  is included in the displacement prediction.

For both rigid and flexible sliding masses, the deterministic approach commonly used in practice underestimates the displacement hazard as compared with the probabilistic approach. The under-prediction becomes more significant for sliding masses with longer periods and for slopes with larger  $k_y$ . The under-prediction is less severe for the vector displacement model than for the scalar displacement model.

A probabilistic approach is required to accurately assess the seismic risk due to slope instability. The probabilistic approach considered in this work incorporates the aleatory variabilities associated with ground shaking, the dynamic response of the slope, and the sliding response of the slope, but it does not incorporate the epistemic uncertainties associated with incomplete knowledge of parameters such as the shear wave velocity and shear strength of the materials in the slope. The effects of epistemic uncertainty can be incorporated using conventional logic tree approaches, in which displacement hazard curves are computed for different sets of input parameters and the hazard curves weighted based on the relative belief in each set of parameters. Including the effects of both aleatory variability and epistemic uncertainty provides a more complete picture of the seismic risk associated with seismic slope instability.

**Acknowledgments** Part of the work presented in this paper was supported by funding from the U.S. Geological Survey (USGS), Department of the Interior, under grants 08HQGR0024 and 06HQGR0057. The views and conclusions contained in this document are those of the authors and should not be interpreted as necessarily representing the official policies, either expressed or implied, of the U.S. Government.

## References

- Baker JW (2007) Correlation of ground motion intensity parameters used for predicting structural and geotechnical response. In: 10th international conference on applications of statistics and probability in civil engineering. Tokyo, Japan
- Bazzurro P (1998) Probabilistic seismic demand analysis, Ph.D. Dissertation. Department of Civil and Environmental Engineering, Stanford University, California, p 329
- Bazzurro P, Cornell CA (2002) Vector-valued probabilistic seismic hazard analysis. In: Proceedings 7th U.S. national conference on earthquake engineering. Boston, MA, p 10

- Boore DM, Atkinson GM (2008) Ground-motion prediction equations for the average horizontal component of PGA, PGV and 5 %-damped PSA at spectral periods between 0.01 s and 10.0 s. *Earthq Spectra EERI* 24(1):99–138
- Bray JD, Rathje EM (1998) Earthquake-induced displacements of solid-waste landfills. *J Geotech Geoenviron Eng Am Soc Civ Eng* 124(3):242–253
- Bray JD, Travasarou T (2007) Simplified procedure for estimating earthquake-induced deviatoric slope displacements. *J Geotech Geoenviron Eng ASCE* 133(4):381–392
- Cornell CA, Luco N (2001) Ground motion intensity measures for structural performance assessment at near-fault sites. In: Proceedings of the U.S.-Japan joint workshop and third grantees meeting, U.S.-Japan cooperative research on Urban earthquake disaster mitigation. Seattle, Washington
- Ghahraman VG, Yegian MK (1996) Risk analysis for earth-induced permanent deformation of Earth dams. In: Proceedings 11th world conference on earthquake engineering, paper 688. Acapulco, Mexico
- Jibson RW (2007) Regression models for estimating coseismic landslide displacement. *Eng Geol* 91:209–218
- Jibson RW, Harp EL, Michael JA (2000) A method for producing digital probabilistic seismic landslide hazard maps. *Eng Geol* 58:271–289
- Lin J, Whitman R (1986) Earthquake induced displacements of sliding blocks. *J Geotech Eng ASCE* 112(1):44–59
- Makdisi FI, Seed HB (1978) Simplified procedure for estimating dam and embankment earthquake induced deformations. *J Geotech Eng Div Am Soc Civ Eng* 104(7):849–867
- Rathje EM, Antonakos G (2011) A unified model for predicting earthquake-induced sliding displacements of rigid and flexible slopes. *Eng Geol* 122:51–60. doi:[10.1016/j.enggeo.2010.12.004](https://doi.org/10.1016/j.enggeo.2010.12.004)
- Rathje EM, Bray JD (2001) One and two dimensional seismic analysis of solid-waste landfills. *Can Geotech J* 38:850–862
- Rathje EM, Saygili G (2008) Probabilistic seismic hazard analysis for the sliding displacement of slopes: scalar and vector approaches. *J Geotech Geoenviron Eng ASCE* 134(6):804–814
- Rathje EM, Saygili G (2009) Probabilistic assessment of earthquake-induced sliding displacements of natural slopes. *Bull N Z Soc Earthq Eng* 42:18–27
- Rathje EM, Saygili G (2011) Pseudo-probabilistic versus fully probabilistic estimates of sliding displacements of slopes. *J Geotech Geoenviron Eng ASCE* 137(3):208–217. doi:[10.1061/\(ASCE\)GT.1943-5606.0000431](https://doi.org/10.1061/(ASCE)GT.1943-5606.0000431)
- Rathje EM, Faraj F, Russell S, Bray JD (2004) Empirical relationships for frequency content parameters of earthquake ground motions. *Earthq Spectra Earthq Eng Res Inst* 20(1):119–144
- Saygili G, Rathje EM (2008) Empirical predictive models for earthquake-induced sliding displacements of slopes. *J Geotech Geoenviron Eng ASCE* 134(6):790–803
- Travasarou T, Bray JB, Der Kiureghian A (2004) A probabilistic methodology for assessing seismic slope displacements. In: Proceedings 13th world conference on earthquake engineering, paper 2326. Vancouver, Canada
- Vrymoed JL, Calzascia ER (1978) Simplified determination of dynamic stresses in earth dams. In: Proceedings, earthquake engineering and soil dynamics conference, ASCE, NY, pp 991–1006
- Yegian MK, Marciano EA, Ghahraman VG (1991a) Seismic risk analysis for Earth dams. *J Geotech Eng ASCE* 117:18–34
- Yegian MK, Marciano EA, Ghahraman VG (1991b) Earthquake-induced permanent deformations: probabilistic approach. *J Geotech Eng ASCE* 117:35–50